Robust power management system with generation and demand prediction and critical loads in DC microgrid

Author(s): Esmaeili, Mehdi; Ahmadi, Ali Akbar; Nateghi, Abolfazl; Shafie-khah, Miadreza

Title: Robust power management system with generation and demand prediction and critical loads in DC microgrid

Year: 2023

Version: Accepted manuscript

Please cite the original version:

Esmaeili, M., Ahmadi, A. A., Nateghi, A. & Shafie-khah, M. (2023). Robust power management system with generation and demand prediction and critical loads in DC microgrid. *Journal of Cleaner Production* 384, 135490. https://doi.org/10.1016/j.jclepro.2022.135490

Robust power management system with generation and demand prediction and critical loads in DC microgrid

Mehdi Esmaeili [a], Ali Akbar Ahmadi [a], Abolfazl Nateghi [a], Miadreza Shafie-khah [b]

[a] *Electrical and Computer Engineering Department Kharazmi University, Tehran, Iran*

[b] *School of Technology and Innovations, University of Vaasa, Vaasa, Finland*

Abstract

In this paper, a robust power management system (RPMS) for a DC microgrid is proposed. A novel neural network-based scheme is proposed for the PV cells' generation prediction using ultraviolet (UV) index, temperature, and cloud coverage which gives a considerable improvement in the prediction error in comparison with the existing works. Moreover, another neural network predicts the demand for the microgrid. The proposed RPMS will make decisions under the uncertainties of these prediction errors such that the system stays robust and works near the optimal operating point. Besides, three different possible scenarios for operation of the microgrid are considered which represents all real operating conditions. Then, three corresponding optimization problems are introduced for theses scenarios. Moreover, without loss of generality, load buses are clustered in one critical load bus and three sheddable load buses. The RPMS keeps the critical load bus voltage in a standard range while feeding the maximum possible sheddable buses with 0.9 p.u. voltage or disconnecting them sequentially. The numerical simulation results show the feasibility and effectiveness of the proposed strategy.

1. Introduction

Increasing demand for energy together with environmental concerns makes renewable energy and microgrids hot topics in the last decades. The microgrids usually use solar and wind energy which are clean and freely available and backup energy storage like batteries, as well. By use of the microgrids, the power generation is near to consumers which results in considerably less power loss in transmission lines. Recently, DC microgrids have been gathered much attention in comparison with AC microgrids because of less power loss, easier utilization for dc loads such as electric vehicles and LED lights, no need for synchronization in bus ties connections, and easier integration of DC distributed energy resources (DERs) such as solar photovoltaic (PV), batteries, and fuel cells (Lotfi and Khodaei, 2017).

On the other hand, DERs often have a time-varying and unreliable nature. Thus, a control system is necessary for the load (demand)-generation balance in a microgrid, which needs future demand and generation data. To this end, the control systems use prediction schemes that naturally have prediction errors and add uncertainty in the power management system. In (Chiang et al., 2010) a control system is proposed for an hybrid regenerative power system including photovoltaic and wind power together with combining functions of the grid-tie system and uninterruptible power supply for critical load applications. This control system should manage the error of the prediction in the solar system and wind power. In (Feroldi et al., 2013) an energy management system is propsoed for an hybrid system based on wind-solar power sources and bioethanol. This power management system uses wind-solar power sources to improve reforming efficiency and should ensure a sustainable power supply.

Besides, one of the most important challenges in microgrids is power quality. The generated power should be sufficient and at the desired voltage level. Furthermore, unpredicted outage of the main grid makes it more challenging especially when there are critical loads. These issues together with the dependency of the generation of PV cells and wind turbines to the weather conditions make the control system design more complex (Li, 2010). presents a unique vision for the future of smart transmission grids in which their major features are identified. In this vision, each smart transmission grid is regarded as an integrated system that functionally consists of three interactive, smart components, i.e., smart control centers, smart transmission networks, and smart substations. In (Zhao et al., 2011) a novel planning approach is proposed to meet the need of the more flexible transmission expansion plans, to cope with the increased risks (Saleh et al., 2016). presents the design, control,

Nomenclature

ANN	Artifical neural network
BP	Back propagation method
b_i	Bias vector
C_b^{DC}	Capacitor's capacitance
C_1, C_2	Correlation and cross-correlation matrices
DER	Distributed energy resource
E_b^{DC}	Voltage of the voltage source
G	Irradiance
g	Activation function
i_{PV}	PV cells current
i_o^{PV}	Output current of the DC/DC converter
I_{scr}	Short circuit current in standard test conditions
I_{sc}	Output current at irradiance G and temperature T
i_L^{DC}	Power demand in DC microgrid
LMBP	Levenberg-Marquardt BP
MLP NN	Multi-layer perceptron neural network
$P_{ch}^{ref}(k)$	Reference charge power of the battery
$P_{dis}^{ref}(k)$	Reference discharge power of the battery
$P_{PV}^{ref}(k)$	Reference power of PV cells
$P_{Batt}^{ref}(k)$	Reference power of the battery
P_{ch}^{max}	The maximum rate of charge
P_{dis}^{max}	The maximum rate of discharge
$P_D(k)$	Predicted demand power
P_{PV}^{P}	Predicted power generated by PV cells
PV	Photovoltaic
ΔP_{PV}	Error in prediction of PV cells' power generation
ΔP_D	Error in prediction of the demand power
P_{Net}^{ref}	Injected power by the main grid
$P_{CLB}^{ref}(k)$	Reference power in the critical load bus
$P_{SLB_i}^{ref}$	Reference power in the shedding load bus i
R	Resistance load of the microgrid
RPMS	Robust power management system
R_b^{DC}	Internal resistance of the voltage source
s	Activation function
Sn	Sun duration
T	Temperature
UV	Ultra violet index
u_{PV}	Control signal of PV cells
$V_{CLB}(k)$	Voltage of the critical load bus
$V_{SLB_i}(k)$	Voltage of the shedding load bus i
$V_{DC}(k)$	DC bus voltage
V_{DC}^{max}	DC bus voltage maximum bound
V_{DC}^{min}	DC bus voltage minimum bound
v_{PV}	PV cells voltage
v_b^{DC}	DC voltage of the battery bank
v_c^{DC}	Capacitor's voltage
W_i	Weight matrices
x_n	Normalized value of the data
x_a	Actual value of the data
x_m	Minimum value of the data
x_M	Maximum value of the data
β	Temperature coefficient
α_i	Some positive constants
ρ	Correlation coefficient

energy management, and implementation of the city college of New York DC microgrid laboratory testbed.

In (Hosseinzadeh and Salmasi, 2016), an optimal and robust power management system (RPMS) is proposed for an AC/DC hybrid microgrid that uses PV cells and a wind turbine. It can detect and manage the shading and converter faults in the PV cells and lubricant system failure and converter faults in the wind turbine, as well. This RPMS results in the maximum use of the PV cells and the wind turbines without considering the load shedding problem. Besides, it is assumed all data about the generation of the PV cells and the wind turbine together with the demand in the microgrid is available. (Hosseinzadeh and Salmasi, 2015a) uses the same power management system with a fuzzy control for battery banks.

In (Zhang et al., 2018) a robust model predictive control system is proposed for an islanded microgrid that uses diesel generators, wind turbine, PV cells, sea-water desalination generators and batteries. A two-stage robust model predictive method is proposed to deal with three types of uncertainty scenarios and uncertainty budgets. In (Yanhao et al., 2018) a distributed hierarchical control structure for a DC microgrid is designed based on fuzzy algorithms. The primary and secondary control layers are designed to dynamically change the virtual resistance and eliminate bus voltage deviation. The resource of the micro grid are PV cells, wind turbine, and batteries and it is assumed the micro grid is operated in islanded mode.

In (Jiaqi et al., 2021) a method is proposed for accurate day-ahead hourly forecasting of photovoltaic power. The method combines novel time series forecasting patterns and hybrid deep learning networks and can capture dependencies between time steps and multivariate time series. The optimal memory lengths of models under various prediction horizons affect the forecasting accuracy. In (Zafar et al., 2021) artificial neural networks are used for PV/wind power forecasting. This paper uses a feedforward neural network which is trained by a novel atomic orbital search (AOS) optimization algorithm (Kumar et al., 2022). used artificial neural network and proposed a real-time prediction model for output power prediction of grid-connected semitransparent photovoltaic system.

(Meenal et al., 2022) presents an overview of current and new development of weather forecasting such as solar and wind forecasting techniques for renewable energy systems in smart grids. Many forecasting models such as physical models, statistical models, artificial intelligence-based models, machine learning, and deep learning-based models were discussed. In (Akarslan, 2022) a model based on learning vector quantization is proposed for short-term load demand forecasting. The approach is based on the selection of the best predictor model at each step and around 5.4% improvement is achieved compared to the best individual model. The proposed approach provides more successful results in all combinations using different models. In (Jnr et al., 2021) a hybrid ensemble intelligent model based on wavelet transform, swarm intelligence and artificial neural network is developed. The model is capable of handling high volatility and behavior of time series data and the model produces a forecasting accuracy of 97.5778%. The proposed model has a lower average relative error in comparison to other models.

The weather forecasting available by meteorological organizations is used in some papers to predict power generation (Maknouninejad et al., 2014). presents a cooperative control for distributed generations that uses prediction of the PV cells using weather forecasting. In (Koyama et al., 2012) the problem of optimal voltage and power regulation is formulated for distributed generators in DC microgrids. It is shown that the resulting control is optimal but would require the full information of the microgrid (Maknouninejad et al., 2012). uses weather forecast information to predict radiation using a neural network and then, approximates a formula to predict the solar power (Omar Elamine et al., 2015). uses the neural network to predict the amount of electricity that will be produced for the next hour. Besides, a fuzzy logic controller is

Table 1
Comparing the proposed RPMS and other methods.

	The proposed method	(Yanhao et al., 2018)	(Yanhao et al., 2018)	(Hosseinzadeh and Salmasi, 2016)
Microgrid	DC connected	Isolated island AC	Isolated DC	Isolated hybrid AC/DC
Control system	Robust power management system	Robust Model Predictive Control	Dynamic coordinated control strategy	Fault talorent supervisory control
Resources of the microgrid	Main network, PV cells and batteries	Diesel generator, wind turbine, PV cells, sea-water desalination generators and batteris	Wind turbine, PV cells and batteris	Diesel generator, wind turbine, PV cells and batteris
Includes uncertainty	In demand and power generation of PV cells	In resources and loads	None	In power generation of PV cells' and wind turbine
Includes faults	Fault in mian grid	No fault	No fault	Solar and wind sub-system failures

utilized for taking a reasonable decision about storing or selling electricity (Kwasinski and Onwuchekwa, 2011). presents a quantitative method to evaluate DC microgrids availability by identifying and calculating minimum cut sets occurrence probability for different microgrid architectures and converter topologies. Decision-making by the power management systems under these uncertainties is examined by (Holjevac et al., 2015). This paper uses an implementation of model predictive control to reduce the impact of uncertainties (Wu et al., 2015). predicts power demand-generation and uses them to make decisions for the microgrid. An experimental study is also performed in the islanded mode to confirm stable power supply for both AC and DC loads, even in case of considerable power fluctuation of renewable sources and significant power change in the loads. In (Yanhao et al., 2018) A comprehensive isolated island microgrid energy management model and a two-stage robust model predictive control optimization based microgrid operation model is proposed. Three types of data uncertainty are considered in the robust optimization model and several sensitive analysis cases are implemented to evaluate the performance of the proposed model.

The comparsion of different existing methods is summarized in Table 1. It can be conclude from examined papers, there is some gap in the researches and some of them have clear defects. These includes: i) There is no research on RPMS that consider uncertainity in both power generation and load demand; ii) There is large error in power generation prediction in particular in PV cells and solar systems which can affect the PMS performance; iii) There is no robustness in PMSs in case of the main grid fault; iv) There is no maximum power tracking in the solar system without cost of lack of robustness in PMSs.

In this paper, we propose a RPMS scheme based on multiple robust optimization problems to dispatch the power in the microgrid. For this end, three different scenarios are considered and their corresponding RPMS are proposed to determine the power that PV cells, batteries, and the main grid should inject into the microgrid. The goals of RPMS are minimizing the use of the main grid and batteries and maximizing the use of PV cells' power. Besides, without loss of generality, it is assumed that a critical and three sheddable load buses exist in the microgrid. In the case of the main grid outage, the RPMS decreases the voltage level or disconnects the sheddable load buses sequentially to ensure supplying the critical load bus at a standard voltage level. Two neural network-based schemes are utilized for the prediction of the demand and the PV cells power generation. The prediction errors are considered in the demand-generation balance constraints in the related optimization problems and then a RPMS is proposed. The novelties of the paper are: i) a novel neural network-based scheme is proposed for irradiance prediction (which is not available in the meteorological organization's data) and then the PV cells' generation prediction with a considerable less relative error in comparison with the existing works which can help maximum power tracking in the solar system without losing robustness; ii) the demand and generation prediction errors are taken into account in the optimization problems and a robust optimization strategy is proposed which have uncertainties in power generation and demand; iii) a scenario-based power management scheme is proposed to deal with the outage of the main grid and other operating conditions in the microgrid which can supply the demand of the critical loads in case of the main grid fault.

The rest of this paper is organized as follows. Section 2 describes the DC microgrid modeling. In section 3, the proposed RPMS is introduced. Section 5 describe the multi layer perceptron (MLP) and the prediction schemes. The numerical simulation results are shown in section 5 and finally, some concluding remarks are presented in section 6.

2. DC microgrid modelling

In this section, a DC microgrid including PV cells, batteries, DC loads, and converters is considered as illustrated in Fig. 1. The output of PV cells and the battery are connected to the DC bus via two DC/DC converters to control the power flow from PV cells and the charge/discharge process of the battery. Also, the microgrid can connect to the main grid with an AC/DC converter.

It is assumed that the battery is modeled as a voltage source series with a resistance and a capacitor. The mathematical model of output voltage and current of PV cells can be written as (Bevrani et al., 2015):

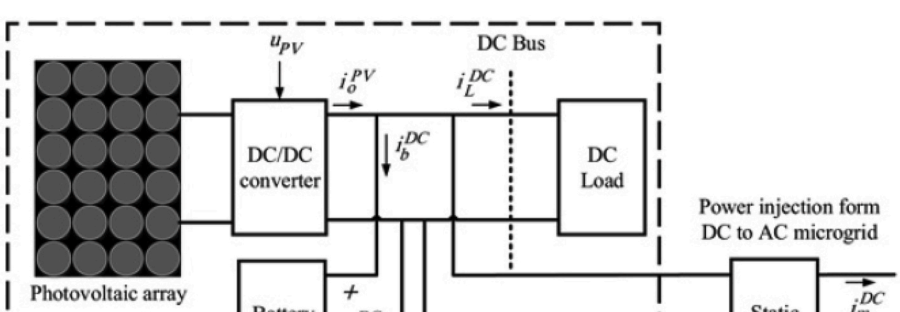

Fig. 1. The DC microgrid (Feroldi et al., 2013).

$$\dot{v}_{PV} = \frac{i_{PV}}{C} - \frac{i_o^{PV}}{C} u_{PV} \quad (1)$$

$$i_o^{PV} = -\frac{v_b^{DC}}{L} + \frac{v_{PV}}{L} u_{PV} \quad (2)$$

$$\dot{v}_c^{DC} = \frac{1}{C_b^{DC}} \left(i_o^{PV} - i_L^{DC} \right) \quad (3)$$

where, v_{PV}, i_{PV}, i_o^{PV}, v_b^{DC}, and u_{PV} are PV cells voltage, PV cells current, the output current of the DC/DC converter, DC bus voltage, and control signal of PV cells, respectively. Moreover, v_c^{DC} and C_b^{DC} are capacitor's voltage and capacitance in the battery model, respectively, C and L are electrical parameters of the DC/DC converter in PV, and i_L^{DC} is the power demand in DC microgrid.

By using (1)-(3), v_b^{DC} can be calculated as follows:

$$v_b^{DC} = E_b^{DC} + v_c^{DC} + \left(i_o^{PV} - i_L^{DC} \right) R_b^{DC} \quad (4)$$

where, E_b^{DC} and R_b^{DC} represent the voltage and internal resistance of the voltage source in the battery model, respectively.

The microgrid must supply the DC loads. It is assumed that the loads are clustered into one critical and three sheddable load buses. The critical load bus is connected to the important loads in the microgrid and must be energized with high priorities. But, three sheddable load buses can tolerate voltage level reduction to 0.9 p.u. and can be disconnected, if necessary.

3. Robust power management system

In this section, the proposed RPMS will be presented for a DC microgrid. The goal of the RPMS is to maximize the use of the PV cells' power and minimize the use of the main grid power to reduce the energy cost. Also, the RPMS should minimize the use of the battery to decrease the charge and discharge time and consequently extend its lifetime. The RPMS should also guarantee the power quality requirements and holds the voltage of the buses in the range of 380–400 V. In the situation of a probable outage of the main grid, the RPMS will decrease the voltage of the not important loads or disconnect them to continuously feed the important loads in the microgrid. It is assumed that decreasing the voltage of the not important loads to 0.9 p.u. will not affect their performance significantly. With these assumptions, there will be three scenarios that the RPMS should handle.

Remark 1. The aforementioned three scenarios include all possible situations that may occur in one DC microgrid which can be connected to the main network. The first and second scenarios represent the islanded and connected operation modes of the microgrid, respectively. The third scenario represents the situation where the DC microgrid should be connected to the main network but there is some faults in the main network and it is not available for at least one time step in the decision-making process (1 h). There is no other situation for a DC microgrid. Thus, these scenarios cover all possible conditions in a DC microgrid operation.

3.1. Scenario 1

In this scenario, it is assumed that the power generated by the PV cells together with the power of the battery is sufficient for supplying the demands. Thus, the RPMS will disconnect the microgrid from the main grid. The RPMS should determine the maximum possible power that the PV cells should deliver to the DC bus and the minimum possible power exchange between the DC bus and battery for supplying all the loads within the acceptable voltage range of 380–400 V. Also, it must be guaranteed that the state of charge (SOC) of the battery remains within the range of 20%–95% to extend its lifetime. The corresponding optimization problem in this scenario can be written as:

$$F_1 : \min\left(\alpha_1 \left(P_{ch}^{ref}(k) + P_{dis}^{ref}(k) \right) - \alpha_2 P_{PV}^{ref}(k) \right) \quad (5)$$

$s.t.$

$$P_{ch}^{ref}(k) - P_{dis}^{ref}(k) + P_{PV}^{ref}(k) + \Delta P_{PV} = P_D(k) + \Delta P_D \quad (6)$$

$$20 \leq SOC(k) \leq 95 \quad (7)$$

$$SOC(k+1) = SOC(k) + \frac{1}{E_{max}} P_{ch}(k) - \frac{1}{E_{max}} P_{dis}(k) \quad (8)$$

$$0 \leq P_{ch}^{ref}(k) \leq P_{ch}^{max} \,, 0 \leq P_{dis}^{ref}(k) \leq P_{dis}^{max} \quad (9)$$

$$V_{DC}^{min} \leq V_{DC}(k) \leq V_{DC}^{max} \quad (10)$$

$$V_{DC}(k) = \sqrt{R * \left(P_{PV}^{ref}(k) + \Delta P_{PV} + P_{Batt}^{ref}(k) \right)} \quad (11)$$

$$\alpha_1, \alpha_2 \geq 0 \quad (12)$$

$$0 \leq P_{PV}^{ref}(k) \leq P_{PV}^{P} \quad (13)$$

where α_1 and α_2 are positive constants, $P_{ch}^{ref}(k)$ and $P_{dis}^{ref}(k)$ are charge and discharge power of the battery, $P_{PV}^{ref}(k)$ is the power that the PV cells should deliver to the DC bus, $P_{Batt}^{ref}(k)$ is the power of the battery which is the summation of $P_{ch}^{ref}(k)$ and $P_{dis}^{ref}(k)$, and P_{ch}^{max} and P_{dis}^{max} are the maximum rate of charge and discharge of the battery, respectively. Moreover, E_{max} is the maximum energy of the battery, $P_D(k)$ is the predicted demand power, and P_{PV}^{P} is the predicted power that PV cells could generate. Moreover, $V_{DC}(k)$, V_{DC}^{max}, and V_{DC}^{min} are the DC bus voltage and its maximum and minimum bounds, respectively. R denotes the load of the microgrid, and ΔP_{PV} and ΔP_D are used to model the error of the PV cells' power generation and demand predictions.

Equation (6) imposes constraints on the demand-generation balance. Besides, (7) and (8) are constraints on the SOC of the battery. The constraint on the power limit of the battery is stated in (9). Moreover, (10) and (11) are constraints on the voltage of the DC bus. The positive constants in (12) can be designed a priori by the system designer.

Remark 2. The terms $P_{ch}^{ref}(k)$ and $P_{dis}^{ref}(k)$ in the cost function 1 which must be positive based on the constraint (9) ensure that either $P_{ch}^{ref}(k) = 0$ or $P_{dis}^{ref}(k) = 0$, $k = 0, 1, 2, \ldots$

It is obvious that F_1 is a convex optimization problem. Thus, its solution is unique and will be the global optimum.

3.2. Scenario 2

In this scenario, it is assumed that the total power generated by the PV cells and the battery is not sufficient for supplying the loads, thus the main grid must be connected to the microgrid. The RPMS should determine the maximum possible power that the PV cells could deliver to the DC bus and the minimum possible power exchange between the DC microgrid and the main grid. moreover, the power of the battery must be minimum. The other constraints are the same as scenario 1. The corresponding optimization problem in this scenario can be written as:

$$F_2 : \min\left(\alpha_1 P_{Net}^{ref} + \alpha_2 \left(P_{ch}^{ref}(k) + P_{dis}^{ref}(k) \right) - \alpha_3 P_{PV}^{ref}(k) \right) \quad (14)$$

$s.t.$

$$P_{ch}^{ref}(k) - P_{dis}^{ref}(k) + P_{PV}^{ref}(k) + \Delta P_{PV} + P_{Net}^{ref}(k) = P_D(k) + \Delta P_D \quad (15)$$

$$20 \leq SOC(k) \leq 95 \quad (16)$$

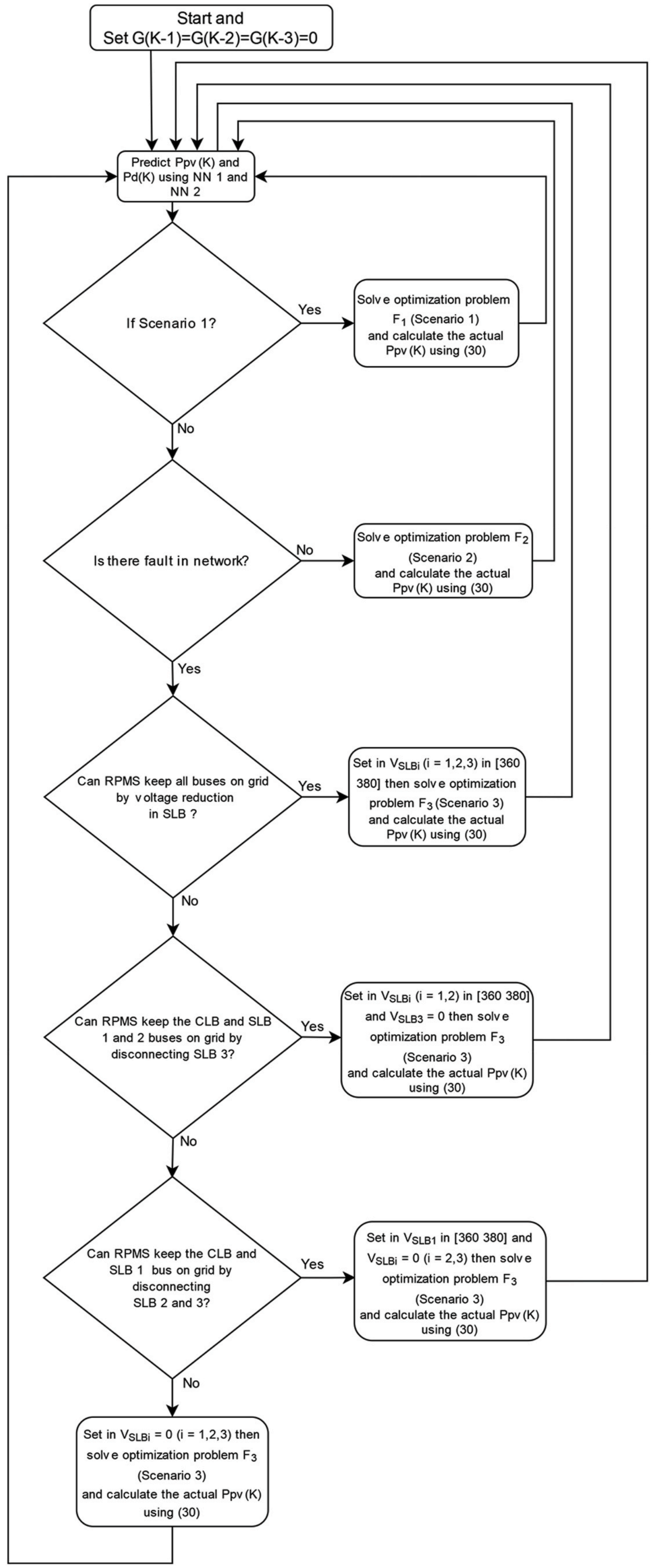

Fig. 2. Flowchart of the proposed PRMS.

$$SOC(k+1) = SOC(k) + \frac{1}{E_{max}} P_{ch}(k) - \frac{1}{E_{max}} P_{dis}(k) \tag{17}$$

$$0 \le P_{ch}^{ref}(k) \le P_{ch}^{max}, 0 \le P_{dis}^{ref}(k) \le P_{dis}^{max} \tag{18}$$

$$V_{DC}^{min} \le V_{DC}(k) \le V_{DC}^{max} \tag{19}$$

$$V_{DC}(k) = \sqrt{R * \left(P_{PV}^{ref}(k) + P_{ch}^{ref}(k) + \Delta P_{PV} - P_{dis}^{ref}(k) + P_{Net}^{ref}(k)\right)} \tag{20}$$

$$\alpha_1, \alpha_2, \alpha_3 \ge 0, \alpha_1 < \alpha_2 \tag{21}$$

$$0 \le P_{PV}^{ref}(k) \le P_{PV}^{P}, P_{Net}^{ref} \ge 0 \tag{22}$$

where P_{Net}^{ref} is a new term added to the cost function which is the injected power by the main grid. This term is added to (15) and (20), as well. The constraint (21) ensures less usage of the battery's power when the microgrid is connected to the main grid.

It is clear that F_2 is also a convex optimization problem.

3.3. Scenario 3

In this scenario, it is assumed that the power generated by the PV cells together with the power of the battery is not sufficient for supplying the loads, and meanwhile, there exists a fault in the main grid and it is disconnected from the microgrid. Also, it is assumed that a critical and three sheddable load buses exist in the microgrid. In this situation, the main priority is to hold the critical load bus voltage in the normal range. At first, the RPMS tries to keep all load buses connected by reducing the voltage of the shedding buses to 0.9 p.u. If it is impossible (the optimization problem is infeasible), the RPMS disconnects the shedding bus 3, decreases the voltage of the shedding bus 1 and 2 to 0.9 p.u., and tries to keep the critical load bus in the normal condition. If it is impossible again, the RPMS will disconnect the next shedding load bus (bus 2) and try again with the critical and shedding bus 1. In this scenario, the power of the PV cells and batteries are set to their maximum possible values and the following optimization problem determines the power that should be inserted into each bus:

$$F_3: \quad \min\left(-\alpha_1 P_{CLB}^{ref}(k) + \sum_{i=1}^{3} \alpha_{i+1} P_{SLB_i}^{ref}(k)\right) \tag{23}$$

$s.t.$

$$P_{batt}^{ref}(k) + P_{PV}^{ref}(k) = P_{CLB}^{ref}(k) + \sum_{i=1}^{3} P_{SLB_i}^{ref}(k) \tag{24}$$

$$P_{batt}^{ref}(k) = P_{dis}^{max} \tag{25}$$

$$V_{CLB}^{min} \le V_{CLB}(k) \le V_{CLB}^{max} \tag{26}$$

$$V_{SLB}^{min} \le V_{SLB_i}(k) \le V_{SLB}^{max} \ or \ V_{SLB_i}(k) = 0, \mathrm{i} = 1,2,3 \tag{27}$$

$$\alpha_1, \alpha_2, \alpha_3, \alpha_4 \ge 0, \alpha_1 \le \alpha_2 \le \alpha_3 \le \alpha_4 \tag{28}$$

$$P_{PV}^{ref}(k) = P_{PV}^{P} \tag{29}$$

where, $P_{CLB}^{ref}(k)$ and $P_{SLB_i}^{ref}, i = 1,2,3$ are the power that should be inserted into the critical load bus and shedding load bus i, respectively. $V_{CLB}(k)$ and $V_{SLB_i}(k), i = 1,2,3$ are the voltage of the critical and shedding load bus i, respectively.

Remark 3. The coefficient $\alpha_i, i = 1,2,3, and\ 4$ are positive constants that show the importance of variables in the cost function. In this work, they are all equal to one but they can be changed in the other works. By increasing one of them, the respective variable must be more reduced to give the optimal solution, if it has a positive sign. Moreover, if we interpret the cost function as the energy price, the coefficient $\alpha_i, i = 1,2,3,4$ would be the operational cost required for generation of 1 KW by the corresponding energy (power) resources. For example, α_1 in (14) would be energy price ratio ($/KW) which be announced by the national or regional electric companies; α_2 in (14) would be the operational and maintenance cost for generation of 1 KW by the PV cells (Nikpour et al., 2021).

The optimization problem F_3 is actually four problems because by disconnecting any of three shedding buses a new problem will be arisen (see the constraint (27)). The constraints (26) and (27) show the different acceptable voltage ranges for the critical and shedding load buses which are assumed to be 380–400 V and 360–380 V (0.9 p.u.), respectively. It is supposed that the loads connected to the shedding buses can operate in 0.9 p.u. voltage without significant effect on their performance (Varaiya et al., 2011).

The constraint (24) is the demand-generation balance. If each shedding bus is disconnected, its corresponding load will be eliminated from this constraint.

The flowchart of the proposed RPMS is illustrated in Fig. 2. The proposed RPMS checks all parameters every hour and determines the scenario. In case of the main grid outage, the RPMS will identify it immediately. After determining the scenarios, the reference values will be computed by solving the corresponding optimization problems, and then the microgrid works with these reference values for an hour.

Remark 4. The RPMS in scenario 3, first checks if it is possible to keep all of the buses connected to the grid with a reduction of the sheddable buses' voltages. This is possible if the optimization problem is feasible with $V_{SLB}^{min} \le V_{SLB_i}(k) \le V_{SLB}^{max}$ in constraint (27). If the problem has no solution, then the RPMS will disconnect sheddable bus 3 ($V_{SLB_3}(k) = 0$) and will solve F_3 again with one critical load bus and two sheddable buses 1 and 2. If the problem has no solution then the RPMS will disconnect the sheddable bus 2 ($V_{SLB_i}(k) = 0, i = 1,2$) and check the problem's solution again. In last if the problem has no solution, the RPMS will disconnect the sheddable bus 3 and only feed the critical load bus. Therefore, at first, it will be specified that the constraint (29) is $V_{SLB}^{min} \le V_{SLB_i}(k) \le V_{SLB}^{max}$ or $V_{SLB_i}(k) = 0, i = 1,2,3$ and then F_3 will be solved.

Remark 5. Three optimization problems $F_i, i = 1,2,3$ have some uncertainties in their constraints. In (Masahiro and Masatoshi, 1995) decision-making under uncertainty is discussed. In (Aumann and Maschler, 1972) the minimax principal in decision-making under uncertainty is examined. In (Dembski, 2009) Bernoulli's principle of insufficient reason and conservation of information in computer search is discussed. (Maghouli et al., 2011) uses a probabilistic model for solving the generation and transmission expansion planning problem and a long-term planning problem in a centralized decision-making framework. In (Zhao et al., 2011) a novel planning approach is proposed. The planning process is modeled as a mixed integer nonlinear programming problem so that conflicting objectives can be optimized simultaneously. In (Hossain et al., 2021) energy management of community energy storage in grid-connected microgrid under uncertain real-time prices are discussed. Scheduling programs demonstrate better performance even under uncertain environments. (Ulansky and Raza, 2021) proposes a new criterion for choosing the optimal decision in a game against nature under a partial a priori uncertainty and also generalizes the Bayes, Wald, Savage, Hurwitz, and Laplace criteria. (Bolurian et al., 2022) presents a new model for day-ahead optimal scheduling of microgrids considering uncertainty by a column and constraint generation optimization algorithm. (Hewitt et al., 2022) proposes a new approach to group scenarios based on the decisions associated with them. This paper introduces a graph structure on the scenarios based on the opportunity cost of predicting the wrong scenario by the decision maker.

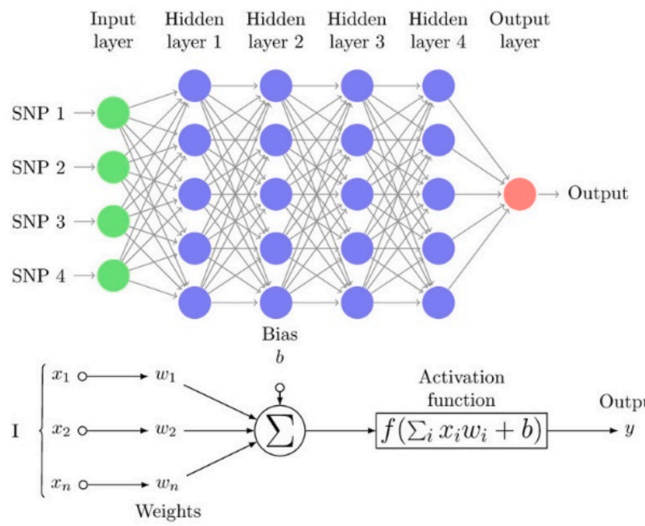

Fig. 3. Schematic representation of a MLP with multiple (the top figure) and single hidden layer (the bottom figure) [Pérez-Enciso and Zingaretti 2019].

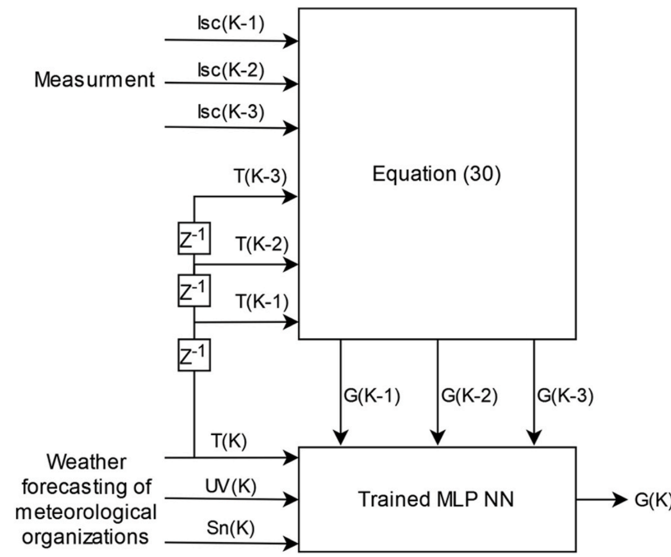

Fig. 4. Block diagram for prediction of the irradiance.

We can classify the aforementioned publications into three approaches (Olatujoye, 2015), (Peng et al., 2015). In the first approach, uncertainties will be ignored and then the optimal solution will be found which results in weak robustness. In the second approach, uncertainties will be considered as a stochastic variable with uniform distribution. In this case, the system work near the optimal point with more robustness in comparison with the first approach. In the third approach, the worst case for uncertainties (the maximum prediction error in our problem) is considered which results in the maximum robustness but performance degradation. This approach is suitable for uncertainties with a small interval. In this paper, since the prediction errors are small values thanks to the proposed prediction scheme, this approach is adopted for robust optimization.

Remark 6. The meaning of maximum prediction error is the maximum absolute error with a negative sign in the PV generation prediction and maximum absolute error with a positive sign in the demand prediction.

In the next section, two schemes will be proposed for prediction of the PV cells' power generation and the demand power. The predicted values will be used as $P_{PV}^{ref}(k)$ and $P_D(k)$, respectively and the prediction error will be considered as $\Delta \boldsymbol{P}_{PV}$ and $\Delta \boldsymbol{P}_D$ in the optimization problems F_1, F_2, and F_3.

4. Prediction schemes

As stated in the previous section, the proposed RPMS needs information about the demands and generated power by the PV cells. Thus, a prediction scheme is needed to give this information. In the following, the neural network structure and the prediction scheme are introduced.

4.1. Multi-layer perceptron

Multi-layer perceptron (MLP) is a supplement of feed-forward neural network. It consists of three types of layers: the input layer, output layer, and hidden layer, as shown in Fig. 3. The input layer receives the input signal to be processed. The required task such as prediction and classification is performed by the output layer. An arbitrary number of hidden layers that are placed in between the input and output layer is the computational engine of the MLP. Similar to a feed-forward NN, in a MLP the data flows in the forward direction from the input to the output layer. The neurons in the MLP are trained with the backpropagation (BP) learning algorithm. MLPs are designed to approximate any continuous function and can solve problems that are not linearly separable. The major use of MLP are pattern classification, recognition, prediction, and approximation.

The computations take place at every neuron in the output and hidden layer as follows (Abirami, 2020)

$$o(x) = g(b_2 + W_2 h(x))$$

$$h(x) = s(b_1 + W_1 x)$$

for a NN with one hidden layer, where b_1, b_2 are bias vectors; W_1, W_2 are weight matrices and g and s are activation functions. The set of parameters to learn is $\theta = \{W_1, b_1, W_2, b_2\}$. Typical choices for g and s include *tanh* function $\left(tanh = \frac{(e^a - e^{-a})}{(e^a + e^{-a})}\right)$ or logistic *sigmoid* function $\left(sigmoid = \frac{1}{(1+e^{-a})}\right)$.

4.2. Prediction of the PV cells' generation

In the proposed RPMS, it is necessary to know the amount of available power in the microgrid. The power of the batteries is known but the information about the PV cells' power generation is not available since it depends on the weather conditions.

The output current of the PV cells can be obtained by (Vandenberghe, 2004):

$$I_{sc} = \left(\frac{G}{G_r}\right) I_{scr}[1 + \beta(T - T_r)] \tag{32}$$

where I_{scr} is short circuit current in standard test conditions, I_{sc} is output current at irradiance G and temperature T, and β is temperature coefficient. If the voltage is supposed to be constant, the power of the PV cells can be calculated by (32). Therefore, to predict the power generated by the PV cells, it is sufficient to predict the temperature and irradiance. The overall prediction scheme is depicted in Fig. 4. The temperature can be easily obtained from the weather prediction from the meteorological organizations because of its high precision. But, the irradiance is not available for 24 h a day. Thus, it should be predicted by other weather parameters received from the meteorological organizations. Moreover, it should be determined which parameters have a significant effect on the irradiance. For this end, a correlation analysis is performed. In the correlation analysis, the linear relationship between a dependent parameter and other independent parameters is examined as follows:

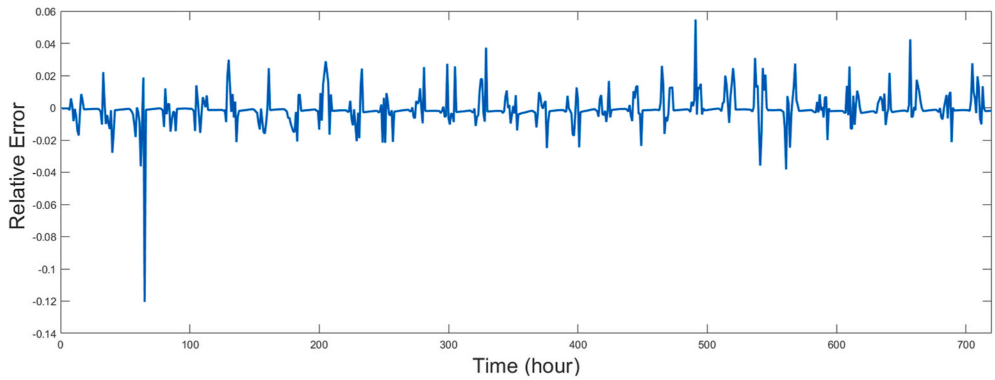

Fig. 5. Relative error of irradiance prediction.

$$C_1 = \begin{bmatrix} \rho(G(k), G(k)) & \cdots & \rho(G(k), G(k-m)) \\ \vdots & \ddots & \vdots \\ \rho(G(k-m), G(k)) & \cdots & \rho(G(k-m), G(k-m)) \end{bmatrix}$$

$$C_2 = \begin{bmatrix} \rho(G(k), G(K)) & \rho(G(K), T(K)) & \rho(G(K), UV(K)) & \rho(G(K), Sn(K)) \\ \rho(T(K), G(K)) & \rho(T(K), T(K)) & \rho(T(K), UV(K)) & \rho(T(K), Sn(K)) \\ \rho((UV(K), G(K))) & \rho(UV(K), T(K)) & \rho(UV(K), UV(K)) & \rho(UV(K), Sn(K)) \\ \rho(Sn(K), G(K)) & \rho(Sn(K), T(K)) & \rho(Sn(K), UV(K)) & \rho(Sn(K), Sn(K)) \end{bmatrix}$$

where C_1 and C_2 are auto-correlation and cross-correlation matrices with entries in [-1 1], respectively. Variables T, UV, and Sn are temperature, UV index, and sun duration, respectively.

Remark 7. The 24-h irradiances often are not available by meteorological organizations and thus should be predicted. On the other hands, the past irradiance values can be obtained from the actual power generated by the PV cells (which is a known data) and some calculations using (32). Once the actual irradiance values are obtained in an acceptable time window, C_1 and C_2 and consequently the most relevant parameters to the irradiance can be identified. Finally, these parameters and the actual value of irradiances are used to train a multi-layer perceptron (MLP) neural network.

4.3. Demand prediction

The demand in the electric networks usually has a pattern that is repeated every year. Therefore, the best way for predicting the demand is based on its past values.

In this paper, the proposed method in (Barghinia et al., 2001) is adopted for demand prediction. At first, each week is divided into four clusters: Saturday, workdays (Sunday to Wednesday), Thursday, and Friday. This is because of the same pattern of loads on these days. It is worth noting that this clustering could be changed based on the load patterns in every region or country. For each cluster, a MLP neural network with four layers is used, separately. The past demand values that have a significant effect on the demand of 1-h ahead are identified by the correlation analysis for each cluster, separately. These values together with temperature data are considered the inputs of the neural networks. This scheme results in a 2% relative prediction error. Since the demand prediction is not the main contribution of this paper, we do not present more explanations. For more details, see (Barghinia et al., 2001).

Remark 8. PV cells' generation and demand are two time series. As we know, ANNs can be used for time series prediction in different area. Thus, without loss of generality, we used this method for prediction of PV cells' generation and load demand. The demand prediction uses a four -ayer perceptron. Levenberg-Marquardt BP (LMBP) method has been used for the artificial neural network (ANN) training to increase the speed of convergence. This method is proposed in 2001 and is old but has acceptable performance and low error (2% relative error) which is important for us. This method can be replaced with any newer method with lower error. The prediction method is not important in this paper, since the relative error is finally considered in the optimization process as ΔP_D, which depends on the relative error regardless of the method of the prediction. (Rafi et al., 2021) and (Kunjin Chen et al., 2019) are articles about newly proposed methods for short-term load forecasting. In (Rafi et al., 2021) a short-term load forecasting model by integration of convolutional neural network and long short-term memory network is proposed considering the real-time electricity price. (Kunjin Chen el. al. 2019) presents a model for forecasting the short-term electric load based on deep residual networks.

Remark 9. The wind turbine and other renewable power sources can be added to the microgrid. Designing a RPMS in presence of such power sources are within the future scope of our works.

5. Simulation results

In this section, simulation results for the operation of a DC microgrid with the proposed RPMS are performed for a typical day. It is assumed that there is a power outage of the main grid in 8–9 AM. Also, the uncertainties in the prediction are considered as the uncertain parameter taking its worst-case value. Therefore, the maximum and minimum values for ΔP_{PV} and ΔP_D will be considered, respectively. It is assumed that bus 1 is the critical load bus, and buses 2, 3, and 4 are shedding buses. Without loss of generality, it is assumed that the demand for each of these buses is equal to a quarter of the predicted demand.

The PV cells have 40 parallel strings and 10 series-connected modules per string. The maximum power of each module is 213.5 Watt. Also, the battery is lithium-ion and its rated voltage is 380 V and has a 30 Ah rated capacity with a 5 kW/h maximum rate of charge/discharge. The simulations are run on Intel (R) Xeon 3.8 GHz CPU, and 64 GB of RAM. All the simulations are performed using the MATLAB/Simulink package, and the optimization problems are solved by linear programming

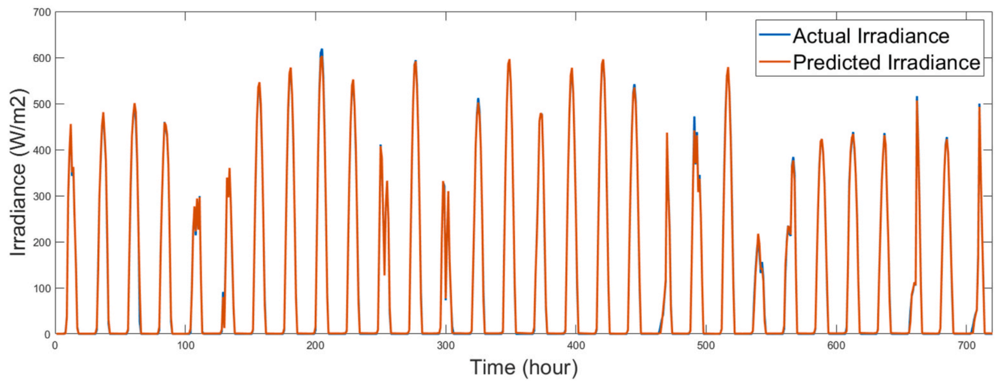

Fig. 6. Actual and predicted irradiance for our proposed method.

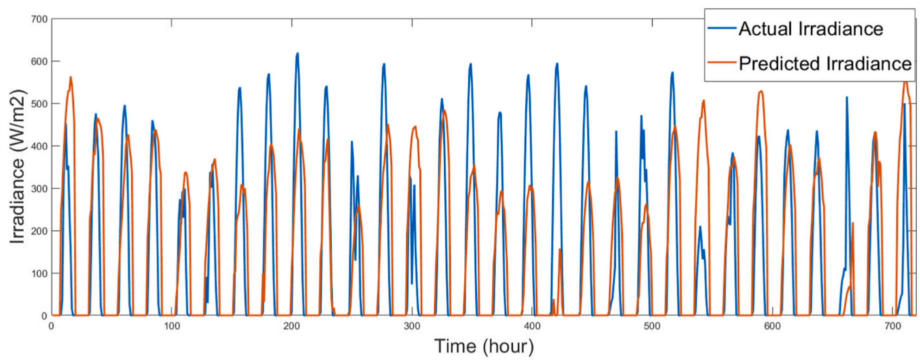

Fig. 7. Actual and predicted irradiance by applying the method in [26].

(linprog) Toolbox (Grant and Boyd, 2013).

Before running the optimization problems, the neural network for the prediction of the irradiance and consequently the power of PV cells will be trained. For this end, parameters that have the most effect on the irradiance will be distracted from the correlation analysis. At first, the correlation between the present irradiance and its past values is checked out. The irradiance is a dynamical parameter and its values change continuously and have a tough relation with its past values. The following matrix shows the correlation analysis result:

$$C_1 = \begin{bmatrix} 1 & 0.9058 & 0.7045 & 0.4533 \\ 0.9058 & 1 & 0.9058 & 0.7045 \\ 0.7045 & 0.9058 & 1 & 0.9058 \\ 0.4533 & 0.7045 & 0.9058 & 1 \end{bmatrix}$$

The result reveals that there is a high correlation between the present irradiance and its three last hours values. Besides, a correlation analysis is also necessary on the other weather parameters such as humidity, temperature, UV index, and sun duration because these parameters can directly influence the irradiance. The result is shown in the below matrix which reveals that there is high correlation between the irradiance, the temperature, the UV index, and the sun duration.

$$C_2 = \begin{bmatrix} 1 & 0.3909 & 0.9680 & 0.8875 \\ 0.3909 & 1 & 0.3703 & 0.3237 \\ 0.9680 & 0.3703 & 1 & 0.7824 \\ 0.8875 & 0.3237 & 0.7824 & 1 \end{bmatrix}$$

Now, a MLP neural network with three layers is used to estimate the mapping between the inputs (the irradiance, the temperature, the UV index, the sun duration, the irradiance in one, two, and 3 h ago) and the output (the irradiance value in 1 h ahead). Each hidden layer has seven neurons. For training the neural network, the data are collected from the Mehr-Abad weather station (Irradiation data). The data are normalized in [−1 1] as follows to speed up the convergence rate of the neural network in the training process:

Table 2
Comparing the proposed method in this paper and other methods.

	The proposed method	(Sharma et al., 2011)	Kim et al. (2017)
Prediction Models	MLP NN	Regression/Support Vector Machine (SVM)	Regression/ SVM
Period of prediction	hourly	daily	daily
Average percentage error for one month	0.5	19.3	10.7

$$x_n = \frac{x_a - x_m}{x_M - x_m} \times 2 - 1 \tag{33}$$

where x_n, x_a, x_m, and x_M are normalized, actual, minimum, and maximum values of the data, respectively. Fig. 5 shows the relative prediction error for this neural network for a month (720 h in one month) which is 12% at maximum. In (Sharma et al., 2011), the daily irradiance is predicted with 25% maximum relative prediction error. Then, this prediction values are used for prediction of the PV cells' generation which its RMS error is 163 $watts/m^2$. This RMS error reaches 193 $watts/m^2$ if the method is applied directly for hourly prediction. The RMS error in our proposed method in this paper is 5 $watts/m^2$. Figs. 6 and 7 show the actual and predicted irradiance for our proposed method and the method in (Sharma et al., 2011). There are two reasons for this considerable improvement. First, in (Sharma et al., 2011) the average values of the weather conditions are used in the daily prediction scheme. Consequently, sudden changes in the weather conditions reduce the precision of the daily prediction scheme which use the average values. Changing the period from one day to 1 h increase the prediction error from 163 $watts/m^2$ to 193 $watts/m^2$. The second reason is in our proposed prediction method we also predict weather changes by using

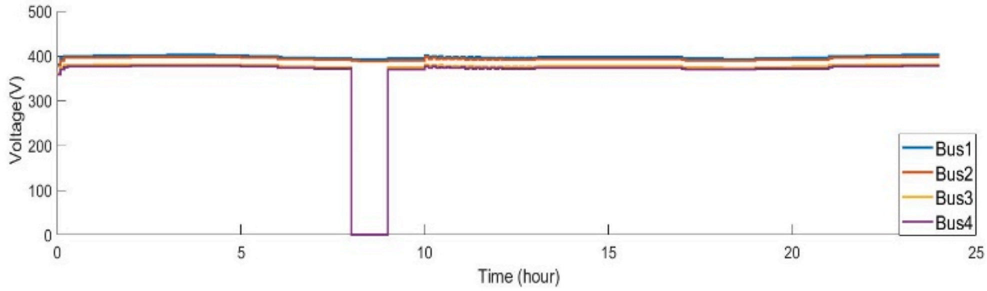

Fig. 8. The voltage of the buses (Bus1: V_{CLB}, Bus2: V_{SLB_1}, Bus3: V_{SLB_2}, and Bus4: V_{SLB_3}).

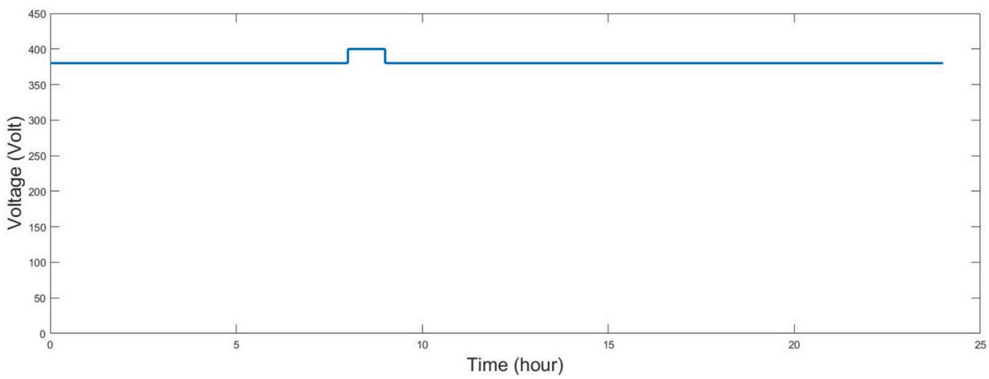

Fig. 9. The commands of the RPMS for voltage of the critical load bus (V_{CLB}).

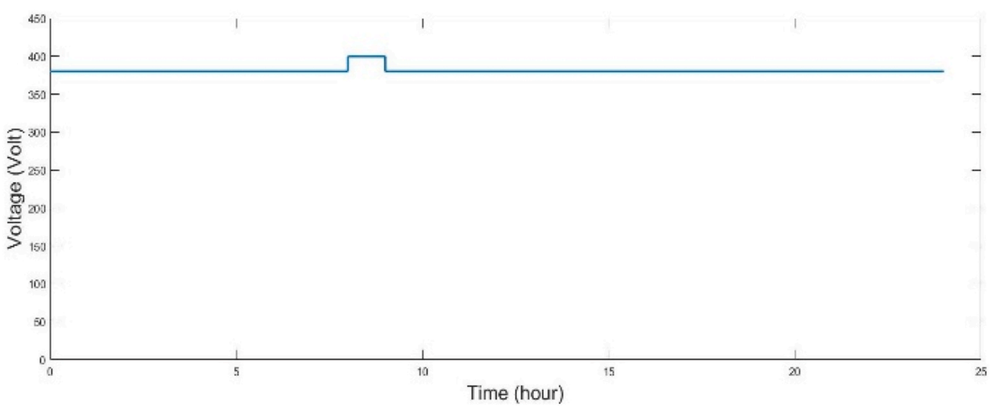

Fig. 10. The commands of the RPMS for voltage of the shedable load bus 1 (V_{SLB_1}).

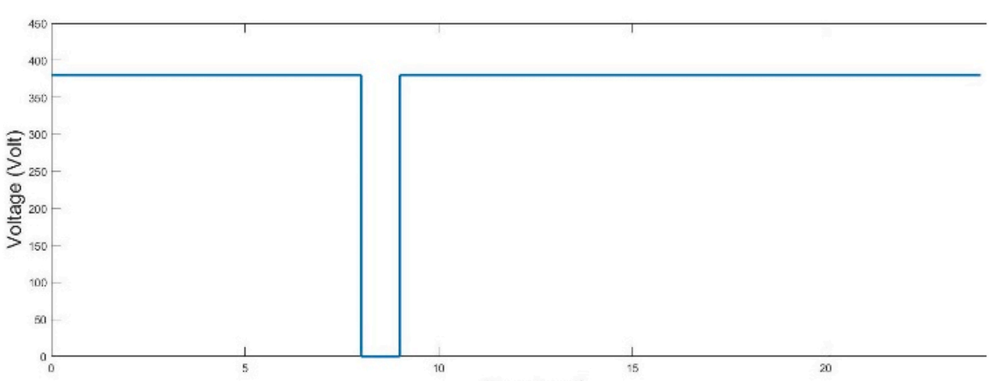

Fig. 11. The commands of the RPMS for voltage of the shedable load bus 2 (V_{SLB_2}).

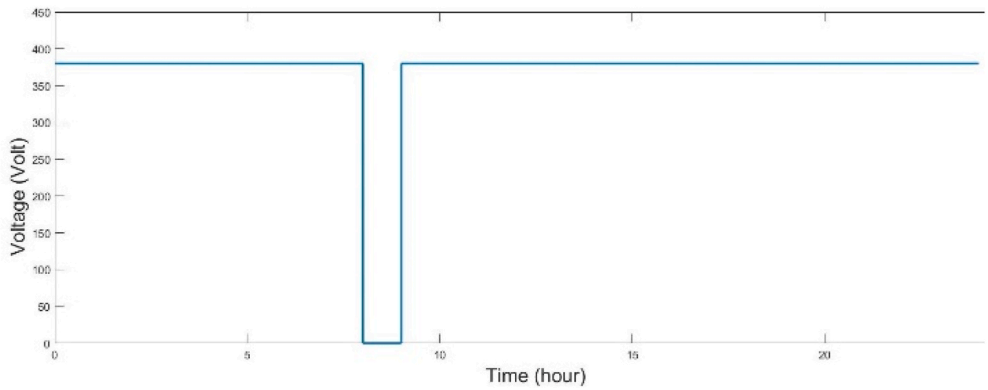

Fig. 12. The commands of the RPMS for voltage of the shedable load bus 3 (V_{SLB_3}).

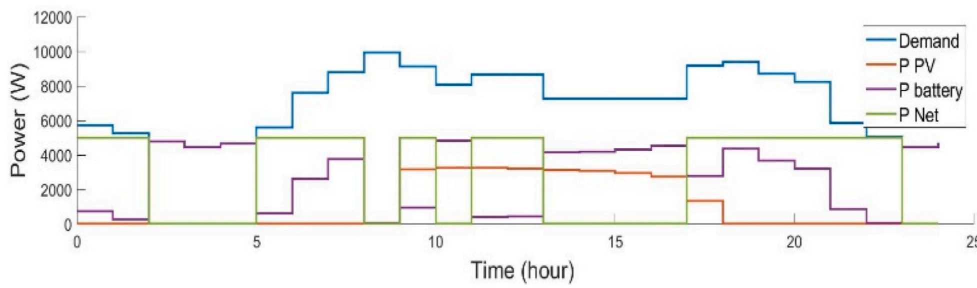

Fig. 13. The demand and the sent commands of the PRMS to the main grid, PV cells, and battery.

weather forecast parameters like sun duration. Further, our proposed method predicts the irradiance with higher precision than the method in (Sharma et al., 2011) because of using parameters like UV index and past irradiance.

In (Kim et al., 2017), the proposed method predicts the power generation of PV cells using past irradiance and weather forecast. Thus, this method needs a sensor to measure the irradiance. This proposed method has typically 10.7%–23.6% average prediction error in one month that may reach 65.5% in some days. Our proposed method has 0.5% average prediction error that reaches 12% in some days (see Table 2). Besides, our proposed method does not need any sensor to measure the irradiance and calculates it using (32).

Finally, 1-h ahead power generation of the PV cells can be predicted by this predicted irradiance and (32) with high precision. Reducing the prediction error allows us to easily use the third approach for dealing with the uncertainties in the optimization problems in the proposed RPMS and keeps it near to the optimal point with good robustness.

Fig. 8 depicts the voltage of all buses. The result shows that the voltage of the critical load bus (bus 1) remains within 380–405 V in presence of the outage of the main grid. Moreover, the shedding load bus 1 is also energized with a similar voltage to the critical load bus. But the shedding load buses 2 and 3 have been disconnected during the outage of the main grid. Then we can see that the RPMS could keep the critical load bus on and satisfy its voltages issues (the 380 V to 400 V bands) during the main grid fault and also keep two of the shedding load buses by decreasing their voltages according to the shedding bus voltages issues during the fault (360 V to 380 V).

The commands of the RPMS for voltage of the buses are depicted in Figs. 9–12 which show the commands for critical load bus and sheddable load bus1, 2, and 3. By these commands the critical load and sheddable load buses should have 380 V and 400 V in normal operation and sheddable load bus under the outage of the main grid, respectively. Also,

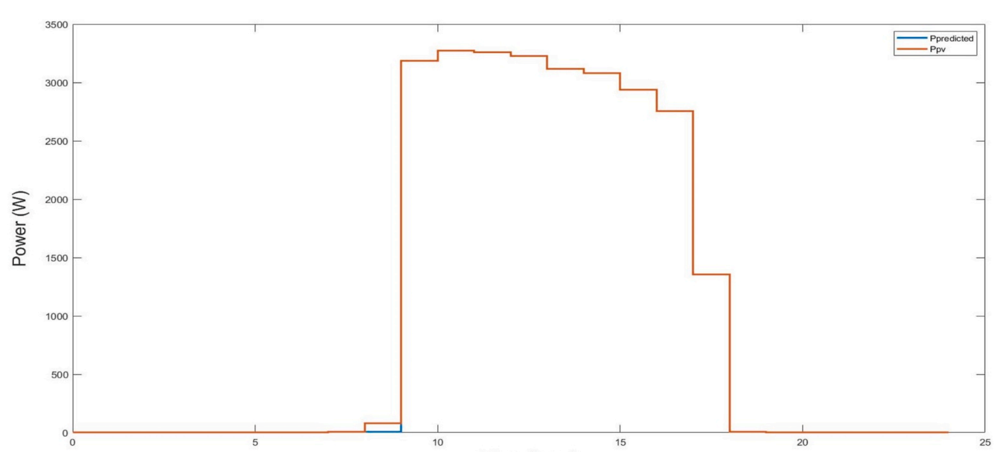

Fig. 14. The prediction of the power generation of the PV cells (blue line) and the actual power generated by PV cells (red line).

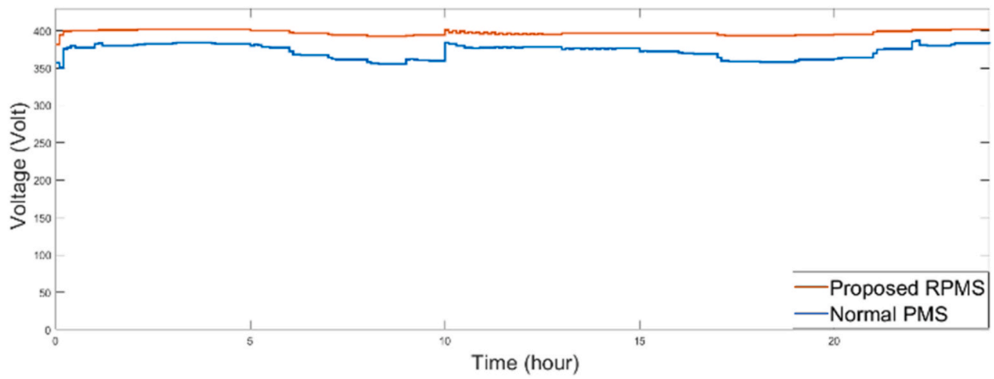

Fig. 15. The voltage of the critical load bus in proposed RPMS and voltage of the all buses in normal PMS.

by these commands the shedding load buses 2 and 3 should be disconnect during the outage of the main grid and have 380 V during the normal operation. These commands will be sent to the DC/DC converter of each bus. The demand power and power produced by each source are shown in Fig. 13. The demand is 5278 W in the start then reaches 8780 W during the outage of the main grid. The maximum demand is 9952 W during 8–9 a.m. The power that should be produced by PV cells' is near 0 until the 9 a.m. At 9 a.m. it is 3185 W and this gets to its maximum, 3272 W, at 10 a.m. From 5 p.m. to 6 p.m., this is 1356 W and then by sunset its go near the zero in the remaining hours. The command of the main grid's converter is 5000 W when the RPMS is in scenario 2 (12 a.m.–2 a.m., 5 a.m.–8 a.m., 9–10 a.m., 11 a.m. to 1 p.m., and 5 p.m.–11 p.m.) and 0 when it is in scenario 1 and 3. The command for the batteries's converters is 4794 W at 2 a.m.–3 a.m. which is equal to the demand in scenario 1. This power reaches to 4811 W at 10 a.m. to satisfy the demand. When the RPMS is in scenario 2 (12 a.m.–2 a.m., 5 a.m.–8 a.m., 9–10 a.m., 11 a.m. to 1 p.m., 5 p.m.–11 p.m.) it varies from 260 W to 4381 W.

The prediction of the power generation of the PV cells and the actual power of PV cells are illustrated in Fig. 14. The power prediction of PV cells is same as the converter of the PV cells. The actual power produced by PV cells is 0 until the 8 a.m. It is equal to 78 W in 8 a.m. It is 3158 W in 9 a.m. and reaches to 3272 W in 10 a.m. As shown in Figs. 11 and 12, the maximums available power by the PV cells is used by the RPMS.

If we compare Figs. 13 and 14 which show the commands of RPMS to PV cells and the predicted power of the PV cells, we can see the RPMS uses near the maximum power of the PV cells which was one of the RPMS goals. The error of the prediction of the PV cells' power directly influences the use of the maximum power of the PV cell because the RPMS commands to use the maximum available PV cells power (as illustrated in Figs. 13 and 14) based on the predicted available power by NN. Then as much as the error be low, the maximum power tracking of the RPMS will happen.

Also, the RPMS minimized the use of the power of the main grid and the battery (unless in case of the main grid fault) to decrease the cost of energy and extend the life of the batteries which was the other goal of the RPMS. In Fig. 13, it is illustrated except during the main grid fault time (8 a.m.–9 a.m.) the RPMS keeps the use of the power of the batteries and main grid as low as possible.

Remark 10. The voltage of the critical load bus and sheddable bus 1 in Fig. 8 have exceeded 400 V because of the uncertainty approach used in the RPMS. The RPMS solves the problem for the worst case, i.e., the maximum absolute error with a negative sign in the PV generation prediction and the maximum absolute error with a positive sign in the demand prediction. Thus, if the actual power generated by the PV or the actual demand is increased or decreased from their prediction values, respectively, the voltage will exceed 400 V, but this error is negligible (approximately 5 V in 400 V).

After these results, another simulation was processed. In this simulation, the effect of the scenarios and the robustness of the RPMS is examined. Therefore, a simple PMS is proposed that has no scenario and has only one cost function same as (16). This PMS just tries to minimize the use of the main network and maximize the use of PV cell's power and has no plan for the main network fault. Also, the uncertainties considered as a stochastic variable with uniform distribution (second approach). Fig. 15 shows the voltages of all buses for simple PMS (they have the same voltage and the voltages vary from 350 to 380 V) and the voltage of the critical load bus in our proposed RPMS (it varies from 380 to 405 V). Therefore, there is a degradation in voltages of the buses in the simple PMS method which is unacceptable at the load side particularly in critical loads. But, in our proposed RPMS the voltage of the critical load bus remains in the acceptable boundary. There are two reason for this degradation in voltage in the simple PMS method. First, in the 8–9 a.m. the main network has a fault and is not available therefore the batteries and PV cells are the sources that can be used. But, in 8 a.m. the PV cells can't produce enough power and load must be supplied by batteries in which is not enough for all loads. This leads to degradation in voltage in 8 a.m.–9 a.m. Second, uncertainties in PV cells' power prediction and demand prediction are considered as stochastic variable with uniform distribution which cause mismatch between the generated power and load demand. If predictions have higher error and uncertainties have bigger interval this mismatching will be increased and the shift in the voltage of the buses will be more. In the other hand, the worst case for uncertainties (the maximum prediction error) which used in our proposed method, leads to more robustness in voltage in comparison to other approach. The small intervals of the uncertainties caused the maximum power tracking of the PV cells' power in our proposed RPMS.

6. Conclusion

In this paper, a scenario-based RPMS for a DC microgrid is proposed to maximize the use of the PV cells and minimize the use of the main grid and the battery. Using a shedding scheme in the corresponding optimization problems, voltage of the critical loads is maintained in the acceptable range in the off-gride mode. Besides, A novel neural network-based method is proposed for prediction of the irradiance and consequently the PV cells' power generation with superior accuracy in comparison with the existing results. The proposed scheme does not need the irradiance data which may not be available by the meteorological organizations.

For practical implementation of the proposed approach and in particular the prediction system of the PV cells' power, the required meteorological is available by www.weather.com website. This data is required for daily work of the prediction system but also, there is a need for data about one year of meteorological and demand data of the region to train the power and demand prediction neural networks. Therefore, there is a need for a powerful computer that can handle the neural network training task. Also, the computer should handle the hourly computation of the optimizations in RPMS. For the implementation of the RPMS, there is a need for bi-directional converters which can control the input or output power by a signal command from RPMS. Furthermore, there should be voltage, current, and power measurement equipment to determine the power of each source for hourly prediction scheme (32).

Applying the proposed scheme for a hybrid microgrid is in the scope of our future works.

References

Abirami, S., Chitra, P., 2020. Adv. Comput. 117, 339–368.

Akarslan, E., 2022. Learning Vector Quantization based predictor model selection for hourly load demand forecasting. Appl. Soft Comput. 117.

Aumann, R.J., Maschler, M., 1972. Some thoughts on the minimax principle. Manag. Sci. 18 (5), 4–63.

Barghinia, S., Ansarimehr, P., Habibi, H., Vafadar, N., 2001. Short term load forecasting of Iran national power system using artificial neural network. In: IEEE Porto Power Tech Proceedings (Portugal), pp. 1–5.

Bevrani, H., Feizi, R., Ataee, M., 2015. Robust frequency control in an islanded microgrid: H_∞ and μ-Synthesis approaches. IEEE Trans. Smart Grid 7 (2), 1527–1532.

Bolurian, A., Akbari, H., Mousavi, S., 2022. Day-ahead optimal scheduling of microgrid with considering demand side management under uncertainty, Electr. Power Syst. Res. 209.

Chen, K., Chen, K., Wang, Q., He, Z., Hu, J., 2019. Short-term load forecasting with deep residual networks. In: IEEE Trans. Smart Grid, vol. 10, pp. 3943–3952, 4.

Chiang, H.C., Ma, T.T., Cheng, Y.H., Chang, J.M., Chang, W.N., 2010. Design and implementation of a hybrid regenerative power system combining grid-tie and uninterruptible power supply functions. IET Renew. Power Gener. 4 (1), 85–99.

Dembski, W., Marks II, R., 2009. Bernoulli's principle of insufficient reason and conservation of information in computer search. In: Proceedings of the IEEE International Conference on Systems, Man, and Cybernetics San Antonio. TX, USA.

Elamine, D.O., Nfaoui, E.H., Jaouad, B., 2015. Multi-agent system based on fuzzy control and prediction using NN for Smart microgrid energy management. Intelligent Systems and Computer Vision (ISCV) Morocco 1–6.

Feroldi, D., Degliuomini, L.N., Basualdo, M., 2013. Energy management of a hybrid system based on wind-solar power sources and bioethanol. Chem. Eng. Res. Des. 91 (8), 1440–1455.

Grant, M., Boyd, S., 2013. CVX: Matlab Software for Disciplined Convex Programming beta, version 2.0. http://cvxr.com/cvx.

Hewitt, M., Ortmann, J., Rei, W., 2022. Decision-based scenario clustering for decision-making under uncertainty. Ann. Oper. Res. 315 (2), 747–771.

Holjevac, N., Capuder, T., Kuzle, I., 2015. Adaptive control for evaluation of exibility benefits in microgrid systems. Energy 92 (3), 487–504.

Hossain, M.A., Chakrabortty, R.K., Ryan, M.J., Pota, H.R., 2021. Energy management of community energy storage in grid-connected microgrid under uncertain real-time prices. Sustain. Cities Soc. 66, 102658.

Hosseinzadeh, M., Salmasi, F.R., 2015a. Power management of an isolated hybrid AC/DC micro-grid with fuzzy control of battery banks. IET Renew. Power Gener. 9 (5), 484–493.

Hosseinzadeh, M., Salmasi, F.R., 2016. Fault-tolerant supervisory controller for a hybrid AC/DC micro-grid. IEEE Trans. Smart Grid 9 (4), 2809–2823.

Irradiation of Mehr-Abad weather station 1990 to 2010. https://meteonorm.com/en.

Jiaqi, Q., Zheng, Q., Yan, P., 2021. Day-ahead hourly photovoltaic power forecasting using attention-based CNN-LSTM neural network embedded with multiple relevant and target variables prediction pattern. Energy 232, 1–18.

Jnr, E., Ziggah, Y.Y., Relvas, S., 2021. Hybrid ensemble intelligent model based on wavelet transform, swarm intelligence and artificial neural network for electricity demand forecasting. Sustain. Cities. Soc. 66, 1–13.

Kim, J., Kim, D., Yoo, W., Lee, J., Kim, Y., 2017. Daily prediction of solar power generation based on weather forecast information in Korea. IET Renew. Power Gener. 11 (10), 1268–1273.

Koyama, M., Takeda, T., Yukita, K., Goto, Y., Ichiyanagi, K., Goda, T., 2012. Operation method of microgrid using the forecast method by neural network. IEEE International Telecommunication Energy Conference (INTELEC) Japan. 818–823.

Kumar, P.M., Saravanakumar, R., Karthick, A., 2022. Artificial neural network-based output power prediction of grid-connected semitransparent photovoltaic system. Environ. Sci. Pollut. Res. 29 (7), 10173–10182.

Kwasinski, A., Onwuchekwa, C.N., 2011. Quantitative evaluation of dc microgrids availability: effects of system architecture and converter topology design choices. IEEE Trans. Power Electron. 26 (3), 835–851.

Li, F., 2010. Smart transmission grid: vision and framework. IEEE Trans. Smart Grid 1 (2), 168–177.

Lotfi, H., Khodaei, A., 2017. AC versus DC microgrid planning. IEEE Trans. Smart Grid 8 (1), 296–304.

Maghouli, P., Hosseini, S., Oloomi Buygi, M., Shahidehpour, M., 2011. A scenario-based multi-objective model for multi-stage transmission expansion planning. IEEE Trans. Power Syst. 26 (1), 470–478.

Maknouninejad, A., Lin, W., Harno, H.G., Qu, Z., Simaan, M.A., 2012. Cooperative control for self-organizing microgrids and game strategies for optimal dispatch of distributed renewable generations. Energy Syst 3 (1), 23–60.

Maknouninejad, A., Qu, Zh, Lewis, F.L., Davoudi, A., 2014. Optimal, nonlinear and distributed designs of droop controls for DC microgrids. IEEE Trans. Smart Grid 5 (5), 2508–2517.

Masahiro, I., Masatoshi, S., 1995. Minimax regret solution to linear programming problems with an interval objective function. Eur. J. Oper. Res., Elsevier 86 (3), 526–536.

Meenal, R., Binu, D., Ramya, K.C., 2022. Weather forecasting for renewable energy system: a review. Arch. Comput. Methods Eng. 29, 2875–2891.

Nikpour, A., Nateghi, A., Shafie-khah, M., Catalao, J.P.S., 2021. Day-ahead optimal bidding of microgrids considering uncertainties of price and renewable energy resources. Energy 227, 120476.

Olatujoye, O.A., 2015. Uncertainty in Power System Planning. Ph. D. Dissertation. Iowa State University.

Peng, C., Lei, S., Hou, Y., Wu, F., 2015. Uncertainty management in power system operation. CSEE J. Power and Energy Syst. 1 (1), 41–62.

Rafi, S.H., Deeba, S.R., Hossain, E., 2021. A short-term load forecasting method using integrated CNN and LSTM network. In: IEEE Access, vol. 9, pp. 32436–32448.

Saleh, M., Esa, Y., Mhandi, Y., Brandauer, W., Mohamed, A., 2016. Design and Implementation of CCNY DC Microgrid Testbed. IEEE Industry Applications Society Annual Meeting, Portland OR, pp. 1–7.

Sharma, N., Sharma, P., Irwin, D., Shenoy, P., 2011. Predicting solar generation from weather forecasts using machine learning. IEEE International Conference on Smart Grid Communications (SmartGridComm) 528–533.

Ulansky, V., Raza, A., 2021. Generalization of minimax and maximin criteria in a game against nature for the case of a partial a priori uncertainty. Heliyon 7 (7), e07498.

Vandenberghe, L., 2004. Convex Optimization. Cambridge University Press, Cambridge.

Varaiya, P.P., Wu, F.F., Bialek, J.W., 2011. Smart operation of smart grid: risk-limiting dispatch. Proc. IEEE 99 (1), 40–57.

Wu, G., Ono, Y., Alishahi, M., 2015. Development of a resilient hybrid microgrid with integrated renewable power generations supplying DC and AC loads. In: Proc. IEEE International Telecommunications Energy Conference (INTELEC) Japan, pp. 1–5.

Yanhao, H., Si, Y., Yang, M., 2018. Multi-source dynamic coordinated control strategy for DC microgrid based on fuzzy control. In: 2nd IEEE Conference on Energy Internet and Energy System Integration (EI2), pp. 1–6.

Zafar, M.H., Khan, N.M., Khan, U.A., 2021. Short term hybrid PV/wind power forecasting for smart grid application using feedforward neural network (FNN) trained by a novel atomic orbital search (AOS) optimization algorithm. International Conference on Frontiers of Information Technology (FIT) 72–77.

Zhang, Y., Fu, L., Zhu, W., Bao, X., Liu, C., 2018. Robust model predictive control for optimal energy management of Island microgrids with uncertainties. Energy 164, 1229–1241.

Zhao, J., Dong, Z., Lindsay, Wong, K., 2011. Flexible transmission expansion planning with uncertainties in an electricity market. IEEE Trans. Power Syst. 24 (1), 479-4.